

# Dalton Transactions

Accepted Manuscript



This is an *Accepted Manuscript*, which has been through the Royal Society of Chemistry peer review process and has been accepted for publication.

*Accepted Manuscripts* are published online shortly after acceptance, before technical editing, formatting and proof reading. Using this free service, authors can make their results available to the community, in citable form, before we publish the edited article. We will replace this *Accepted Manuscript* with the edited and formatted *Advance Article* as soon as it is available.

You can find more information about *Accepted Manuscripts* in the [Information for Authors](#).

Please note that technical editing may introduce minor changes to the text and/or graphics, which may alter content. The journal's standard [Terms & Conditions](#) and the [Ethical guidelines](#) still apply. In no event shall the Royal Society of Chemistry be held responsible for any errors or omissions in this *Accepted Manuscript* or any consequences arising from the use of any information it contains.

Cite this: DOI: 10.1039/c0xx00000x

www.rsc.org/xxxxxx

ARTICLE TYPE

# Pt NPs immobilized on core-shell magnetite microparticles: a novel and highly-efficient catalyst for the selective aerobic oxidation of ethanol and glycerol in water

Yu Long, Kun Liang, Jianrui Niu, Bing Yuan, Jiantai Ma\*

Received (in XXX, XXX) Xth XXXXXXXXX 20XX, Accepted Xth XXXXXXXXX 20XX  
DOI: 10.1039/b000000x

Three core-shell structures were prepared with pyrrole, glucose, and tetraethyl orthosilicate (TEOS) respectively, encasing magnetic Fe<sub>3</sub>O<sub>4</sub> microparticles, through three different “green” approaches without any toxic solvents. Pt nanoparticles (NPs) were immobilized onto these supports with NaBH<sub>4</sub> as reducing agent. The as-prepared catalysts were characterized thoroughly by TEM, VSM, XRD, FT-IR, ICP, and XPS. As expected, the shells remarkably affected the distribution of Pt NPs and catalytic activity. Pt NPs evenly dispersed evenly on the surface of Fe<sub>3</sub>O<sub>4</sub>@PPy and Fe<sub>3</sub>O<sub>4</sub>@C, which were much better than Fe<sub>3</sub>O<sub>4</sub>@SiO<sub>2</sub>. Most attractively, the prepared catalysts exhibited better kinetics, higher activity and stability than the Pt/Fe<sub>3</sub>O<sub>4</sub> and Pt/C for selective oxidation of ethanol to acetic acid and glycerol to glyceric acid with molecular oxygen in water. Among them, the catalyst with a shell of polypyrrole (PPy) showed the best catalytic property, affording yields of 88% and 55%, respectively. Moreover, it could be recovered facily from the reaction mixture and recycled four times without any significant loss in activity.

## Introduction

The catalytic conversion of biomass and derivatives to chemicals has been the subject of intensive research efforts during the past decade resulting in a 20% annual increase in the number of publications on the subject<sup>1</sup>. The development of catalysts adapted to the processing of each individual feedstock in various biorenewable feedstocks is a big challenge. The oxidation of ethanol to acetic acid<sup>2</sup> and glycerol to glyceric acid<sup>3</sup> with molecular oxygen in water are important reactions for the conversion of biomass to high value chemicals. Many review articles focus on different routes for the transformation of biomass such as biotechnology<sup>4a</sup>, heterogeneous catalytic synthesis<sup>4b</sup>, catalytic steam gasification<sup>4c</sup>, pyrolysis<sup>4d</sup>, using enzymes and cells<sup>4e</sup>, photocatalysis<sup>4f</sup>, metallic catalysts<sup>4g, 4h</sup>. Amongst them, the supported platinum catalysts are the most effective for oxidation of ethanol and glycerol in water, because they do not require the addition of base.

In recent years, various kinds of carrier-supported catalysts have been reported, such as silica<sup>5</sup>, modified MCM-41<sup>6</sup>, zeolites<sup>7</sup> and multi-wall carbon nanotubes (MWCNTs)<sup>8</sup>. However, the separation process is still a challenge, since they are often readily dispersed in the liquid media by Brownian motion. This issue can be solved by using magnetic material such as Fe<sub>3</sub>O<sub>4</sub>, so as to be separated by external magnetic field. Moreover, the surface of Fe<sub>3</sub>O<sub>4</sub> microparticles can be improved by coating chemically modified shells. Thus, interests in preparation of shell coated magnetic materials are increasing dramatically. So far, many different kinds of shells, including SiO<sub>2</sub>, polymer and “carbon”,

are employed to coat magnetic Fe<sub>3</sub>O<sub>4</sub> microparticles<sup>9</sup>. Silica is the most popular inorganic coating material for Fe<sub>3</sub>O<sub>4</sub>, because it is very easily connected to Fe<sub>3</sub>O<sub>4</sub>. Silica as coating shell improves the water solubility and biocompatibility of Fe<sub>3</sub>O<sub>4</sub>. The dense silica shell has plenty of Si–OH groups for potential derivatization with various functional units allowing introduction of catalytic molecules to Fe<sub>3</sub>O<sub>4</sub><sup>9k</sup>. Meanwhile, introducing a shell of polymers with functional groups to the surface of Fe<sub>3</sub>O<sub>4</sub> has been the subject of increasing attention<sup>9l, 9m</sup>. In catalysis, the catalytic performance of can be flexibly tuned and considerably affected by the inherent properties of the polymers, such as solubility, functional groups, degree of cross-linking, hydrophilicity, and hydrophobicity. “Carbon” layer prepared from the glucose precursor can be supposed to be a specific polymer. It possesses functional groups -OH on the surface, which offers an important chemical environment for coordinate with metal NPs. In addition, all of the three shell structures can prevent metal leaching from the core of magnetite particles under harsh shaking conditions<sup>9g</sup>.

However, to our best knowledge, different shells coated Fe<sub>3</sub>O<sub>4</sub> microparticles immobilizing metal NPs had not been compared for catalyzing the same kind of reactions. Herein, we report the successful syntheses of Pt/Fe<sub>3</sub>O<sub>4</sub>@X (X = PPy, C or SiO<sub>2</sub>). Meanwhile, the catalytic properties of these catalysts were compared with the aerobic oxidations of ethanol to acetic acid and of glycerol to glyceric acid. Most importantly, both the preparation and application reactions of the catalysts would not involve toxic or expensive solvents, but in water and alcohol. Furthermore, the magnetic catalysts could be separated and

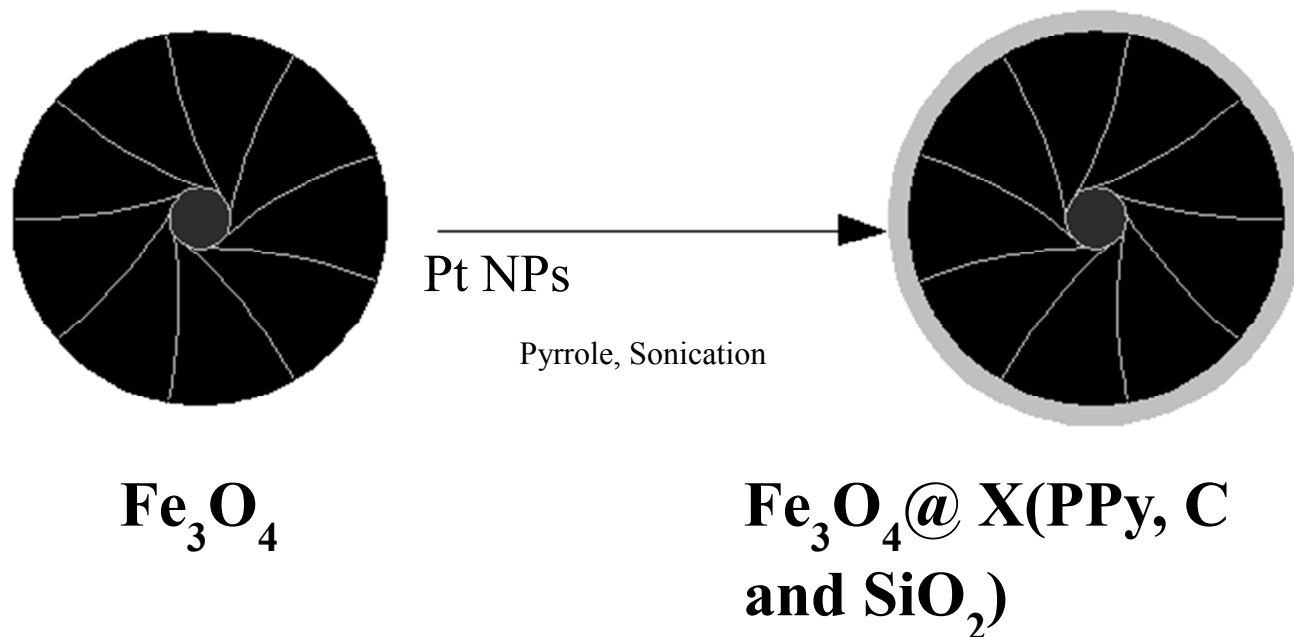
reused by an external magnet.

## Experimental

### Chemicals

Iron (III) chloride hydrate, sodium acetate, Poly-N-vinylpyrrolidone (PVP, K-30), ethylene glycol (EG), pyrrole, glucose, TEOS, potassium chloroplatinate, hexachloroplatinic acid, and 5% Pt/C were purchased from Sigma-Aldrich. Various reaction reagents were purchased from Alfa Aesar. All chemicals were of analytical grade and used as received without further purification. Deionized water was used throughout the experiments.

### Preparation of catalysts



Scheme 1 Preparation of catalysts.

### Synthesis of $\text{Fe}_3\text{O}_4$ microparticles

$\text{Fe}_3\text{O}_4$  microparticles were synthesized with the solvothermal method according to our previous work<sup>9g</sup>. Firstly,  $\text{FeCl}_3 \cdot 6\text{H}_2\text{O}$  (9 g), PVP (6 g) and sodium acetate (12 g) were added into ethylene glycol (200 mL). The mixture was stirred violently for 2 hours to make all materials dissolve completely. Then the mixture was transferred to a Teflon-lined stainless-steel autoclave and sealed to heat at 200 °C for 8 h. The precipitated black products were collected from the solution by an external magnet and washed with deionized water and ethanol several times. Finally, the black products were dried in a vacuum for 24 h at 60°C.

### Synthesis of magnetic $\text{Fe}_3\text{O}_4@PPy$ composites

$\text{Fe}_3\text{O}_4$  microparticles (0.3 g) were dispersed in 70 mL  $\text{H}_2\text{O}$  under sonication, and then pyrrole (4 mL) in ethanol (15 mL) and HCl solution (15 mL, 6 M) were added into the above solution in turn under sonication for 1 h<sup>9c</sup>. Finally, the black product was collected with the help of a magnet, washed with deionized water

and ethanol repeatedly to remove the residual pyrrole monomers and HCl acid, and then dried in a vacuum at 60°C for 12 h.

### Synthesis of magnetic $\text{Fe}_3\text{O}_4@C$ composites

$\text{Fe}_3\text{O}_4@C$  composites were prepared by in-situ carbonization of glucose in the presence of  $\text{Fe}_3\text{O}_4$  microparticles under hydrothermal condition<sup>9d</sup>. Typically,  $\text{Fe}_3\text{O}_4$  microparticles (1 g) were dispersed in hydrochloric acid solution (200 mL, 0.01M) and it was subject to ultrasonic treatment. After 30 min, this material was washed with water and isolated with the aid of a magnet. The resultant material was re-dispersed into water (225 mL) containing glucose (15 g) by ultrasonic decentralize. The mixture was transformed into a Teflon-lined stainless-steel autoclave and the autoclave was placed in an oven and kept at 200 °C for 12 h. After cooled to temperature, the precipitated

deionized water and ethanol several times and finally dried in a vacuum at 60°C for 12 h. The loading level of Pt in the  $\text{Pt}/\text{Fe}_3\text{O}_4@PPy$ ,  $\text{Pt}/\text{Fe}_3\text{O}_4@C$  and  $\text{Pt}/\text{Fe}_3\text{O}_4@SiO_2$  catalyst was measured to be 4.52%, 2.89% and 1.17% by ICP, respectively.

### Characterizations of $\text{Pt}/\text{Fe}_3\text{O}_4@X$ catalyst

These magnetic micro-materials were characterized by transmission electron microscopy (TEM), inductively coupled plasma (ICP), X-ray diffraction (XRD), X-ray photoelectron spectroscopy (XPS), fourier transform-infrared (FT-IR) and vibrating sample magnetometry (VSM). XRD measurements were performed on a Rigaku D/max-2400 diffractometer using Cu-K $\alpha$  radiation as the X-ray source in the 2 $\theta$  range of 10–90°. The size and morphology of the magnetic microparticles were observed by a Tecnai G2 F30 transmission electron microscopy and samples were obtained by placing a drop of a colloidal solution onto a copper grid and evaporating the solvent in air at room temperature. Pt content of the catalyst was measured by ICP on IRIS Advantage analyzer. Magnetic measurements of

Pt/Fe<sub>3</sub>O<sub>4</sub>@X were investigated with a Quantum Design VSM at room temperature in an applied magnetic field sweeping from -8 to 8 kOe. XPS was recorded on a PHI-5702 instrument and the C1s line at 284.8 eV was used as the binding energy reference.

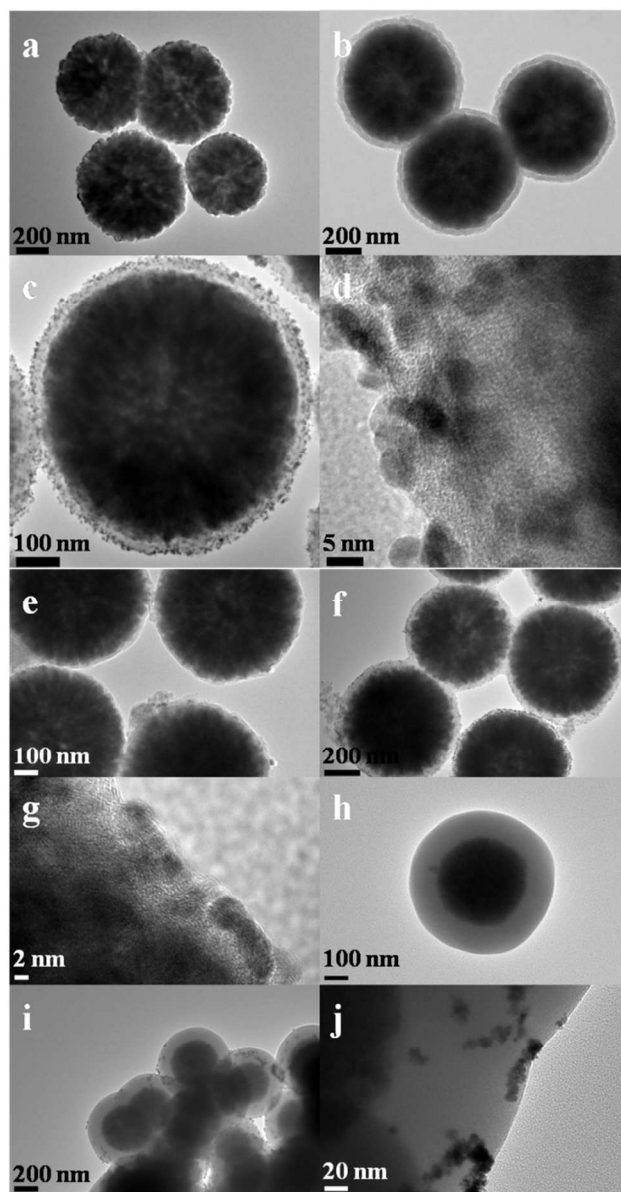
### 5 Catalytic reactions

**Selective oxidation of ethanol.** The catalyst (ethanol/platinum = 200 mol/mol) was dispersed in a solution of 5 wt% ethanol in water (5.0 g). The solution was transferred into a preheated (90 °C) stainless-steel batch reactor (approximate volume 50 mL) with a 30 mL glass insert and immediately pressurized with oxygen (10 bar). Product compositions and concentrations were determined using standard solutions by gas chromatograph (GC). In some cases, the entire reaction mixture was also titrated with aqueous sodium hydroxide after the reaction to validate the GC results. In all cases, the analyses gave identical results within the experimental uncertainties.

**Selective oxidation of glycerol.** The catalyst (glycerol/platinum = 200 mol/mol) was dispersed in aqueous solution of glycerol (5.0 mL, 0.3 M), the following procedure was applied with all tested catalysts. The solution was transferred to a preheated (60 °C) stainless-steel batch reactor (approximate volume 50 mL) and immediately pressurized with oxygen (5 bar). Samples were taken, filtered, and analyzed by high-performance liquid chromatography (HPLC). The proposed method implies the use of a sulfonated divinylbenzene-styrene resin column, which was effective for the analysis with a flow rate of 0.5 mL/min, 3 mM of H<sub>2</sub>SO<sub>4</sub> as mobile phase, and a temperature of 70 °C<sup>3g</sup>.

## Results and Discussion

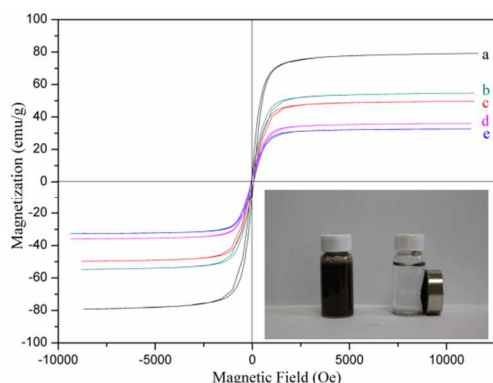
### Characterization of catalysts



30 Fig. 1 TEM images of the prepared materials (a), Fe<sub>3</sub>O<sub>4</sub>; (b), Fe<sub>3</sub>O<sub>4</sub>@PPy; (c) and (d), Pt/Fe<sub>3</sub>O<sub>4</sub>@PPy; (e), Fe<sub>3</sub>O<sub>4</sub>@C; (f) and (g), Pt/Fe<sub>3</sub>O<sub>4</sub>@C; (h), Fe<sub>3</sub>O<sub>4</sub>@SiO<sub>2</sub>; (i) and (j), Pt/Fe<sub>3</sub>O<sub>4</sub>@SiO<sub>2</sub>.

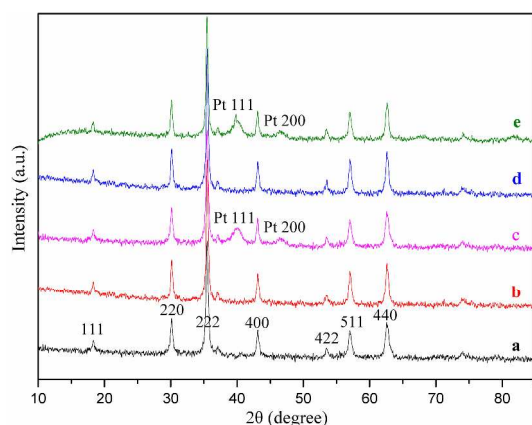
The typical TEM images of Fe<sub>3</sub>O<sub>4</sub> microspheres prepared by the versatile solvothermal reaction are shown in Fig. 1a. The average diameter of the as-synthesized spherical microparticles is about 600 nm. As shown in Fig. 1b, e, h, a continuous layer of PPy, C and SiO<sub>2</sub> can be observed on the outer shell of the Fe<sub>3</sub>O<sub>4</sub> microparticles and the thickness of these shells are about 35 nm, 30 nm, and 150nm, respectively. Meanwhile, the resultant Fe<sub>3</sub>O<sub>4</sub>@X composites have good dispersibility and spherical morphology. In the TEM image of Pt/Fe<sub>3</sub>O<sub>4</sub>@X (Fig. 1c, f, i), it can be seen that the morphologies of Pt/Fe<sub>3</sub>O<sub>4</sub>@X are almost spherical. However, the morphologies of Pt NPs loaded on the surface of different shell materials are different which is out of our expectation. Pt NPs supported on Pt/Fe<sub>3</sub>O<sub>4</sub>@PPy and Pt/Fe<sub>3</sub>O<sub>4</sub>@C disperse well and have uniform particle size centred at 5 nm (Fig. 1c, d, f, g). In contrast, Pt NPs of Pt/Fe<sub>3</sub>O<sub>4</sub>@SiO<sub>2</sub> are not dispersed evenly on the surface and their agglomeration is

obvious (Fig. 1i, j). As a result, Pt/Fe<sub>3</sub>O<sub>4</sub>@SiO<sub>2</sub> with Pt as active centre should not be considered as a good catalyst for any reactions.



5 Fig. 2 VSM of the prepared materials (a), Fe<sub>3</sub>O<sub>4</sub>; (b), Fe<sub>3</sub>O<sub>4</sub>@PPy; (c), Pt/Fe<sub>3</sub>O<sub>4</sub>@PPy; (d), Fe<sub>3</sub>O<sub>4</sub>@C; (e), Pt/Fe<sub>3</sub>O<sub>4</sub>@C.

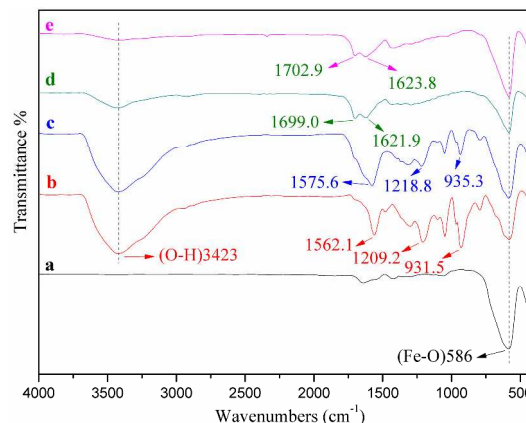
Magnetic measurements are performed using a VSM at room temperature (Fig. 2). The curves show that the five samples are superparamagnetic at room temperature. Therein, Fe<sub>3</sub>O<sub>4</sub>@C and Fe<sub>3</sub>O<sub>4</sub>@PPy show relatively less reduction of the saturation magnetization of Fe<sub>3</sub>O<sub>4</sub> (Fig. 2 b&c). The further decreases of saturation magnetization of Pt/Fe<sub>3</sub>O<sub>4</sub>@C and Pt/Fe<sub>3</sub>O<sub>4</sub>@PPy suggest the presence of platinum particles on the surface of magnetic supports (Fig. 2 d&e). Specifically, the measured saturation magnetization is 36.0 emu g<sup>-1</sup> and 32.7 emu g<sup>-1</sup> for Pt/Fe<sub>3</sub>O<sub>4</sub>@C and Pt/Fe<sub>3</sub>O<sub>4</sub>@PPy, respectively. Even with this reduction in the saturation magnetization, the catalyst can still be efficiently separated from solution with an external magnet as shown in the inset image in Fig. 2.



20 Fig. 3 XRD patterns of the prepared materials (a), Fe<sub>3</sub>O<sub>4</sub>; (b), Fe<sub>3</sub>O<sub>4</sub>@PPy; (c), Pt/Fe<sub>3</sub>O<sub>4</sub>@PPy; (d), Fe<sub>3</sub>O<sub>4</sub>@C; (e), Pt/Fe<sub>3</sub>O<sub>4</sub>@C.

The crystalline structure of the resulting products is investigated by XRD. In Fig. 3 (b, c, d, e), the main peaks of Fe<sub>3</sub>O<sub>4</sub>@PPy, Pt/Fe<sub>3</sub>O<sub>4</sub>@PPy, Fe<sub>3</sub>O<sub>4</sub>@C and Pt/Fe<sub>3</sub>O<sub>4</sub>@C composites are similar to the Fe<sub>3</sub>O<sub>4</sub>. Thus, either the coating of shell or the loading of Pt does not affect the structure of Fe<sub>3</sub>O<sub>4</sub>. All of the five patterns show strong peaks, which confirmed that the products are well-crystallized and the detect diffraction peaks in every pattern could be indexed as cubic Fe<sub>3</sub>O<sub>4</sub> (JCPDS card No. 82-1533). The appearance of two additional peaks (i.e. 2θ = 40 and 46.5) are attributed to the Pt species (Fig. 3 c&e)<sup>9g</sup>. The results

from XRD imply that the Pt NPs have been successfully immobilized on the surface of magnetic microparticles.



35 Fig. 4 FT-IR patterns of the prepared materials (a), Fe<sub>3</sub>O<sub>4</sub>; (b), Fe<sub>3</sub>O<sub>4</sub>@PPy; (c), Pt/Fe<sub>3</sub>O<sub>4</sub>@PPy; (d), Fe<sub>3</sub>O<sub>4</sub>@C; (e), Pt/Fe<sub>3</sub>O<sub>4</sub>@C.

The compositions of all the composite microspheres are confirmed by FT-IR (Fig. 4). As shown in Fig. 4, in the low-frequency region, the vibration bands around 586 cm<sup>-1</sup> correspond to the stretching vibration peak of Fe-O. The vibration bands at 1562.1 cm<sup>-1</sup> (C=C stretching vibrations), 1209.2 cm<sup>-1</sup> (C-N stretching vibrations), and 931.5 cm<sup>-1</sup> (C-H stretching vibrations) reveal the presence of PPy (Fig. 4b). In the spectrum of Pt/Fe<sub>3</sub>O<sub>4</sub>@PPy pattern, it can be concluded that the C=C (1575.6 cm<sup>-1</sup>), C-N (1218.8 cm<sup>-1</sup>), C-H (935.3 cm<sup>-1</sup>) stretching vibrations take place blue shift, which evidence that Pt has been fastened on the support, wherein the N atom is useful for immobilizing Pt NPs. On the other hand, FT-IR spectrum of Fe<sub>3</sub>O<sub>4</sub>@C shows broad bands at 1621.9 cm<sup>-1</sup> and 1699.0 cm<sup>-1</sup> (Fig. 4d), which are assigned to the stretching vibration of COOH, C=O. The characteristic stretch of COOH (1623.8 cm<sup>-1</sup>) and C=O (1702.9 cm<sup>-1</sup>) in Pt/Fe<sub>3</sub>O<sub>4</sub>@C (Fig. 4e) take place blue shift, indicating that coordination reaction have occurred between Pt NPs and ketonic or hydroxyl oxygen on the surface of Fe<sub>3</sub>O<sub>4</sub>@C.

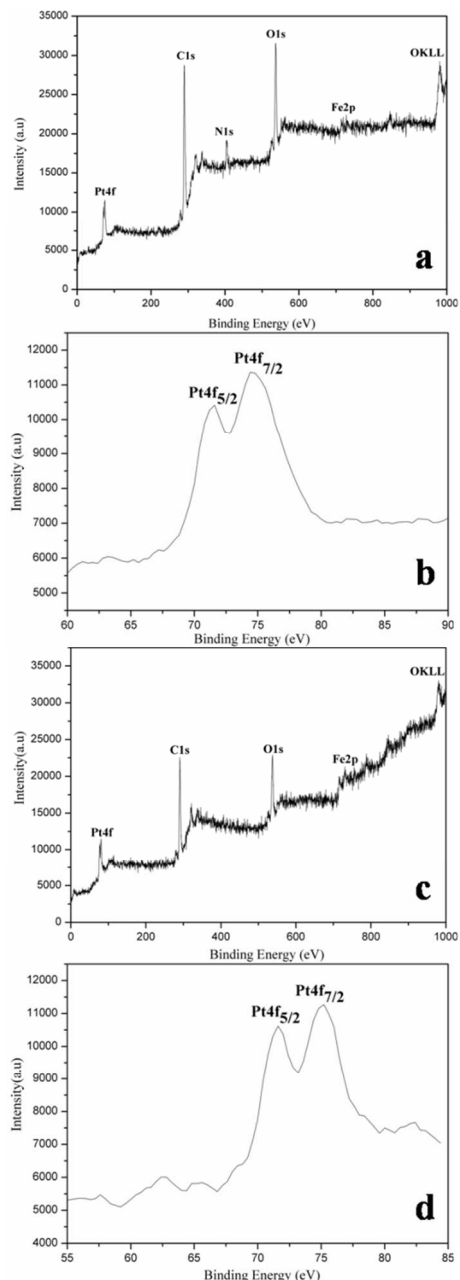


Fig. 5 XPS spectra for the prepared materials (a), Pt/Fe<sub>3</sub>O<sub>4</sub>@PPy; (c), Pt/Fe<sub>3</sub>O<sub>4</sub>@C; and (b, d), showing Pt 4f<sub>5/2</sub>, Pt 4f<sub>7/2</sub> binding energies of Pt/Fe<sub>3</sub>O<sub>4</sub>@PPy, Pt/Fe<sub>3</sub>O<sub>4</sub>@C, respectively.

The XPS elemental survey scans of the surface of the Pt/Fe<sub>3</sub>O<sub>4</sub>@PPy and Pt/Fe<sub>3</sub>O<sub>4</sub>@C are shown in Fig. 5a and c. Peaks corresponding to iron, oxygen, nitrogen, platinum and carbon are clearly observed, indicating the successful preparation of Pt/Fe<sub>3</sub>O<sub>4</sub>@PPy and Pt/Fe<sub>3</sub>O<sub>4</sub>@C. XPS studies are carried out to ascertain the valence state of Pt in the two catalysts. As expected, both the spectra of the Pt 4f region of the two catalysts confirm the presence of Pt (0) with same peak binding energy of 71.2 and 75.2 eV, which are assigned to Pt 4f<sub>5/2</sub> and Pt 4f<sub>7/2</sub>, respectively<sup>9j</sup>. It is a powerful and direct evidence to certify the existence of Pt (0) in both Pt/Fe<sub>3</sub>O<sub>4</sub>@PPy and Pt/Fe<sub>3</sub>O<sub>4</sub>@C. Meanwhile, the peak patterns of the Pt 4f region of the two catalysts are basically similar.

### Catalytic oxidation of ethanol and glycerol

The catalytic activity of the four resultant supported platinum catalysts had been initially investigated in the selective aerobic oxidation of ethanol and glycerol in water. As the structure of the supports are similar and the amount of added platinum in the oxidation reactions are the same (i.e. alcohol/platinum = 200 mol/mol), it is most likely that the different catalytic performances of the catalysts are resulted from the chemical composition of the support. In addition, our catalysts were also compared with Pt/C (5 wt% Pt) catalyst. The platinum-catalyzed oxidation of ethanol and glycerol generally follows a consecutive oxidation mechanism of alcohol to aldehyde to acid with minor formation of CO<sub>2</sub> and other side products<sup>10a</sup>. The mechanisms of platinum-catalyzed oxidation of alcohol have been thoroughly studied<sup>10b-10e</sup>.

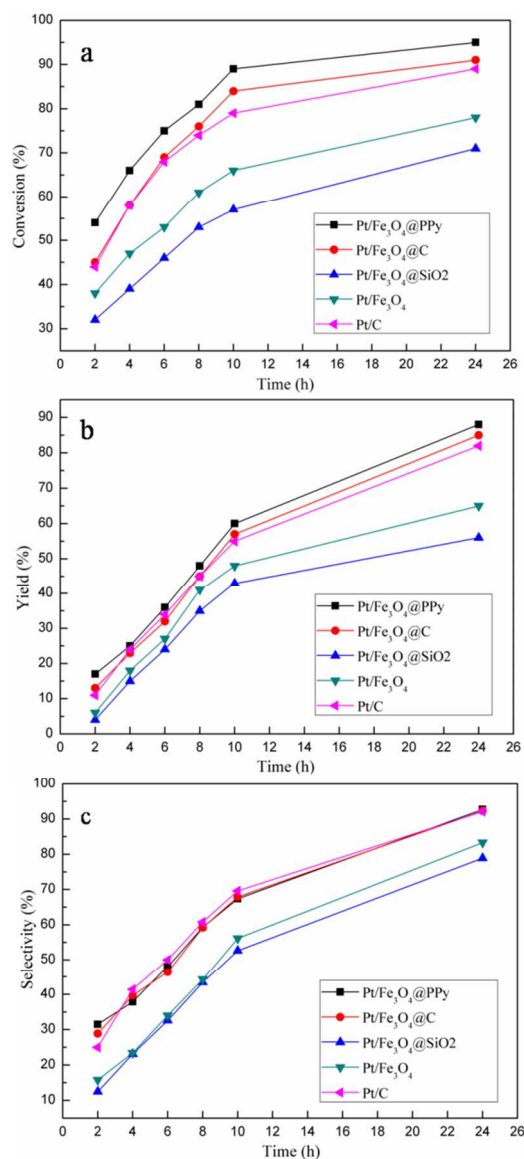


Fig. 6 Comparison of catalysts in the (a) conversion of ethanol, (b) yield of acetic acid and (c) selectivity of acetic acid. Reaction conditions: 5wt% ethanol (aq), ethanol/platinum = 200 mol/mol, oxygen pressure 10 bar, 90°C

### Catalytic oxidation of ethanol

The catalytic activity of these four catalysts and Pt/C catalyst for

oxidation of ethanol is carried out and the results are illustrated in Fig. 6. This reaction is conducted with excessive amount of oxygen. Therefore, the reaction rate mainly obeys pseudo-first-order kinetics, especially in the first ten hours. As shown in Fig. 5 6b, the Pt/Fe<sub>3</sub>O<sub>4</sub>@PPy catalysts affords maximum yield of 88% of acetic acid after 24h reaction time. As expected, Pt/Fe<sub>3</sub>O<sub>4</sub>@SiO<sub>2</sub> has minimum yield of 56% of acetic acid because of the serious agglomeration of Pt NPs on the surface of Fe<sub>3</sub>O<sub>4</sub>@SiO<sub>2</sub>. It is very attractive that all the selectivities of 10 Pt/Fe<sub>3</sub>O<sub>4</sub>@PPy, Pt/Fe<sub>3</sub>O<sub>4</sub>@C, and Pt/C catalysts towards acetic acid are as high as 92.5% (Fig. 6c), which are much higher than those obtained with Pt/Fe<sub>3</sub>O<sub>4</sub> or Pt/Fe<sub>3</sub>O<sub>4</sub>@SiO<sub>2</sub> (i.e. 83.3%&78.9%). On the other hand, through comparing the conversion rates of the ethanol oxidation reaction catalyzed by 15 Pt/Fe<sub>3</sub>O<sub>4</sub>@PPy (95%), Pt/Fe<sub>3</sub>O<sub>4</sub>@C (91%) and Pt/Fe<sub>3</sub>O<sub>4</sub> (78%), we speculate that polymer-supported catalyst are more active than the oxide- and C-supported catalysts. Probably, the coordination of N atom and O atom with Pt NPs accelerate the reaction rate with a more efficient catalytic mechanism than the isolated Pt 20 NPs. Besides that, a fine yield of 82% is also obtained with the catalyst of Pt/C. This may be attributed to the special pore structure and high surface area of Pt/C catalyst (Fig. S1 and Table S1). Hence, Fe<sub>3</sub>O<sub>4</sub>@PPy supported platinum catalyst is a highly efficient catalyst for aerobic oxidation reaction of ethanol and 25 PPy is an excellent choice of the shells of magnetic core-shell structure catalyst.

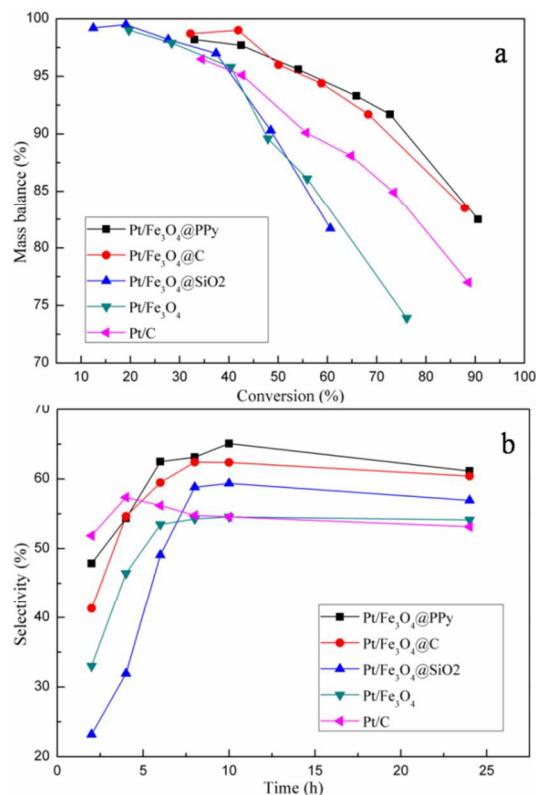


Fig. 7 Comparison of catalysts in the (a) mass balance and (b) selectivity of glyceric acid. Reaction conditions: 0.3 M glycerol (aq), glyceric/platinum = 200 mol/mol, oxygen pressure 5 bar, 60°C.

#### Catalytic oxidation of glycerol

Similarly, Pt/Fe<sub>3</sub>O<sub>4</sub>@PPy still affords the maximum conversion rate of 90.6% of glycerol and the maximum yield of 55.4% of

Table 1 Comparison of catalysts in glycerol oxidation reaction<sup>a</sup>

Cite this: DOI: 10.1039/c0xx00000x

www.rsc.org/xxxxxx

## ARTICLE TYPE

Time (h)	Glycerol conversion (%)	Glyceric acid yield (%)	Glycer-aldehyde yield (%)	Glycolic acid yield (%)	Dihydrox-acetone yield (%)	Glyoxylic acid yield (%)	Tartronic acid yield (%)	Oxalic acid yield (%)	TOF <sup>b</sup> (h <sup>-1</sup> )
<b>Pt/Fe<sub>3</sub>O<sub>4</sub>@PPy</b>									
2	33.0	15.8	11.0	0.9	3.2	1.0	0.5	0.0	33.0
4	42.5	23.1	10.2	1.3	4.9	1.3	0.6	0.1	21.25
6	54.1	33.8	7.2	2.0	6.1	1.4	0.9	0.2	18.03
8	65.9	41.6	6.3	3.1	7.0	1.6	1.7	0.2	16.48
10	72.7	47.3	4.0	4.5	7.3	1.6	1.7	0.3	14.54
24	90.6	55.4	1.3	7.8	7.7	1.1	1.5	0.3	7.55
<b>Pt/Fe<sub>3</sub>O<sub>4</sub>@C</b>									
2	32.2	13.3	13.9	0.7	2.8	0.8	0.3	0.0	32.2
4	41.9	22.9	11.5	1.1	4.0	1.2	0.8	0.0	20.95
6	50.1	29.8	9.2	1.6	4.9	1.4	1.1	0.1	16.7
8	58.8	36.7	7.6	2.1	6.2	1.5	1.3	0.1	14.7
10	68.3	42.6	6.2	3.4	7.1	1.7	1.4	0.2	13.66
24	87.9	53.1	1.9	7.5	7.5	1.6	1.6	0.2	7.33
<b>Pt/Fe<sub>3</sub>O<sub>4</sub>@SiO<sub>2</sub></b>									
2	12.5	2.9	7.9	0.2	1.1	0.2	0.1	0.0	12.5
4	19.1	6.1	9.2	0.6	2.5	0.4	0.3	0.0	9.55
6	27.7	13.6	8.0	1.0	3.2	0.8	0.6	0.0	9.23
8	37.4	22.0	7.1	1.3	4.1	1.1	1.0	0.2	9.35
10	48.5	28.8	5.2	1.7	5.2	1.3	1.3	0.3	9.7
24	60.6	34.5	2.3	2.8	6.9	1.5	1.2	0.3	5.05
<b>Pt/Fe<sub>3</sub>O<sub>4</sub></b>									
2	19.7	6.5	9.9	0.4	1.6	0.6	0.3	0.2	19.7
4	28.4	13.2	9.3	0.7	2.8	0.9	0.6	0.3	14.2
6	40.4	21.6	9.1	1.2	4.4	1.1	0.9	0.4	13.47
8	47.9	26.0	8.0	1.5	5.1	1.4	1.3	0.6	11.98
10	55.9	30.5	6.5	2.1	5.9	1.5	1.7	0.9	11.18
24	76.1	41.2	2.6	3.0	6.9	1.1	1.2	1.3	6.34
<b>5% Pt/C</b>									
2	34.5	17.9	8.8	1.2	3.1	1.2	0.8	0.3	34.5
4	42.7	24.5	8.1	1.6	4.4	1.4	1.1	0.5	21.35
6	55.7	31.3	7.6	2.1	5.9	1.5	1.3	0.5	18.57
8	64.8	35.5	7.0	3.3	7.2	1.9	1.4	0.8	16.2
10	73.5	40.1	5.2	4.2	8.5	1.6	1.6	1.2	14.7
24	88.6	47.1	1.6	6.7	9.4	0.9	0.8	1.7	7.38

a Reaction conditions: 0.3 M glycerol (aq), glyceric/platinum = 200 mol/mol, oxygen pressure 5 bar, 60°C.

b TOF: turnover frequency, i.e., moles of glycerol converted per mole of Pt per hour.

glyceric acid after 24 h reaction time (Table 1). In the oxidation reaction of glycerol catalyzed by Pt/Fe<sub>3</sub>O<sub>4</sub>@PPy, the selectivities towards glycer-aldehyde and glyceric acid are quite high at the initiate stage of reaction (i.e. 11.0% and 15.8% at 2 h reaction time) (Table 1). Additionally, glycer-aldehyde is the intermediate product of glyceric acid. Thus, Pt/Fe<sub>3</sub>O<sub>4</sub>@PPy affords the high selectivity (61.1%) of towards the ultimate product of glyceric acid at 24 h reaction time (Fig 7b). In the comparison between Pt/Fe<sub>3</sub>O<sub>4</sub>@C and Pt/Fe<sub>3</sub>O<sub>4</sub>@PPy, the maximum selectivity and conversion of Pt/Fe<sub>3</sub>O<sub>4</sub>@PPy to glyceric acid are higher (Table 1). The highest selectivity of Pt/Fe<sub>3</sub>O<sub>4</sub>@PPy could be attributed to the interaction between nitrogen and platinum, which has the

potential to selectively block certain active sites responsible for the side reactions. Similarly, the interaction between platinum and oxygen in Fe<sub>3</sub>O<sub>4</sub>@C plays the same role, however, which is less efficient.

As shown in the last column in the table 1, with the increase of reaction time, the turnover frequency (TOF) of each catalyst basically decreased gradually, except for Pt/Fe<sub>3</sub>O<sub>4</sub>@SiO<sub>2</sub>. Since Pt NPs on Pt/Fe<sub>3</sub>O<sub>4</sub>@SiO<sub>2</sub> seriously agglomerate on the surface the change of the TOF catalyzed by Pt/Fe<sub>3</sub>O<sub>4</sub>@SiO<sub>2</sub> might be irregular. It could also be concluded that the reaction rate does not obey pseudo-first-order kinetics. Due to its three hydroxyl groups, the oxidation reaction of glycerol produces many other

by-products such as glyceraldehyde, glycolic acid, dihydroxyacetone, glyoxylic acid, tartronic acid, and oxalic acid. Concerning the oxidation reaction of glycerol, one has to consider a large number of intermediate products and a variety of reaction processes<sup>3a</sup>. The main by-products of platinum-catalyzed reactions are glyceraldehyde, dihydroxyacetone, and glycolic acid of which the former two are interesting substrates toward lactic acid synthesis. The other three measured minor by-products - glyoxylic acid, tartronic acid, and oxalic acid - are observed in traces. The yield of dihydroxyacetone by Pt/Fe<sub>3</sub>O<sub>4</sub>@PPy and Pt/Fe<sub>3</sub>O<sub>4</sub>@C is lower than Pt/C, and Pt/C give the highest yield of oxalic acid. The reason of higher yields of dihydroxyacetone and oxalic acid on Pt/C could be due to its special pore structure and high surface area (Fig. S1 and Table S1). Specifically, the major difference between the catalysts is the yield of by-product glycolic acid, which decreases from polymer to carbon to oxide supports. The higher yields of glycolic acid by Pt/Fe<sub>3</sub>O<sub>4</sub>@PPy and Pt/Fe<sub>3</sub>O<sub>4</sub>@C are partially responsible for the lower quantity of undetectable by-products formed with the catalysts, possibly because the decomposition rate of the products to C1-compounds is lower on the catalysts<sup>10a</sup>. Selectivity toward the other side products is similar for the tested catalysts.

In addition, the mass balance drop slightly with the raise of conversion, which probably due to the formation of CO<sub>x</sub> and other unknown by-products. Overall, reactions catalyzed by Pt/Fe<sub>3</sub>O<sub>4</sub> and Pt/Fe<sub>3</sub>O<sub>4</sub>@SiO<sub>2</sub> have higher loss of mass, probably due to the formation of gaseous products as shown by the largest drop in the determined mass balance at high conversion (Fig. 7a). Conclusively, Fe<sub>3</sub>O<sub>4</sub>@PPy supported platinum catalyst has the best performances amongst all the prepared catalysts in the aerobic oxidation reaction of glycerol. PPy is an excellent choice of the shells of magnetic core-shell structure catalysts. Such conclusion is almost the same with that of ethanol oxidation.

In order to further evaluate the influence of altered chemical compositions of shells on the activities of catalysts in aerobic oxidation reactions, the influence of structure should be excluded. As a consequence, nitrogen adsorption-desorption isotherms of the prepared catalysts and Pt/C catalyst were carried out. As shown in Fig. S1, the nitrogen adsorption-desorption isotherms demonstrate that Pt/Fe<sub>3</sub>O<sub>4</sub>@PPy, Pt/Fe<sub>3</sub>O<sub>4</sub>@C and Pt/Fe<sub>3</sub>O<sub>4</sub>@SiO<sub>2</sub> are nonporous, whereas Pt/C is microporous. We have compared the amounts of Pt and surface area of these catalysts in the aerobic oxidation reactions of ethanol and glycerol (Table S1). It can be concluded that mass fraction of Pt and surface area have no effect on the catalytic activities for the two reactions.

### Catalyst recycling

Furthermore, we investigated the recyclability of the Pt/Fe<sub>3</sub>O<sub>4</sub>@PPy for the aerobic oxidation of ethanol and glycerol in water. After each cycle of the reaction, the catalyst was recovered in the help of an external magnet, and successively washed with distilled water. The recovered catalyst was then subjected to the next catalytic cycle under the same conditions. Pt/Fe<sub>3</sub>O<sub>4</sub>@PPy is a good recyclable catalyst as was shown in Fig. 8a. In the first four cycles, less than 5.3% of activity loss is observed. When we measured the content of platinum in the washing fluid after every reaction, it is found that there are traces of platinum. Thus, the activities of our catalysts decreased quiet

slowly. It is worth noting that the catalyst give an identical selectivity in each cycle without any degradation. The recyclability of Pt/C (5 wt% Pt) is also measured, which is compared with our catalyst Pt/Fe<sub>3</sub>O<sub>4</sub>@PPy (4.52 wt% Pt). As shown in Fig. 8b, the conversions of the two alcohols degraded at the similar rate in the presence of both catalysts. However, the selectivities of both oxidation reactions of ethanol and glycerol descend obviously. Conclusively, our catalyst maintains a very well catalytic activity, especially the selectivity in multiple recycle reactions. Furthermore, the recycling process is very simple and the Pt/Fe<sub>3</sub>O<sub>4</sub>@PPy catalysts are facily separated from the reaction medium by magnetic decantation.

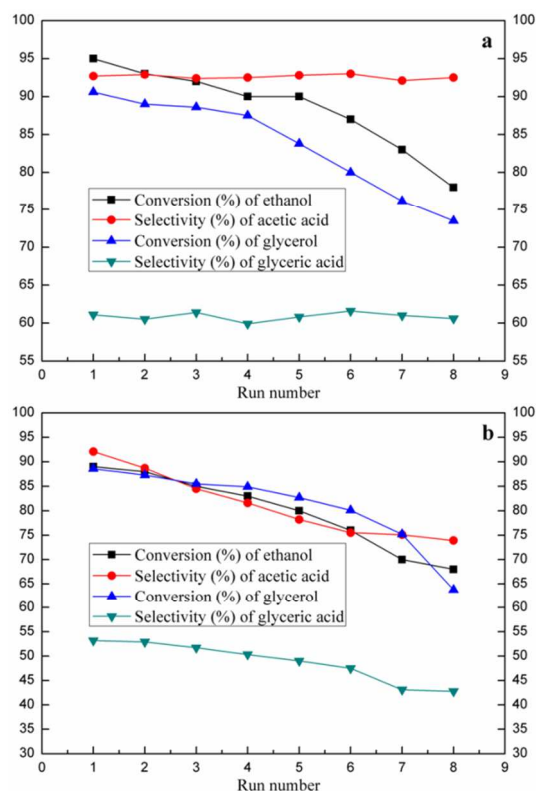


Fig. 8 Recycling study of the prepared catalysts (a), Pt/Fe<sub>3</sub>O<sub>4</sub>@PPy; (b), 5% Pt/C in oxidation reaction of ethanol and glycerol

### Conclusion

In summary, we have successfully prepared four catalysts consisting of different shells with excellent magnetism, good crystallinity and dispersibility. This study compares the catalytic properties of the catalysts and Pt/C in the aerobic oxidation of ethanol and glycerol in water. Fe<sub>3</sub>O<sub>4</sub>@PPy supported platinum catalyst shows the best catalytic activity, not only the highest conversion but also the best selectivity. Hence, PPy is an excellent choice of the shells of magnetic core-shell structure catalysts for the two reactions. Moreover, the catalyst exhibits high stability in the recycling reactions. Our catalyst has shown great advantages since toxic or expensive solvents are avoided in both of the preparation and application reactions. Additionally, our catalyst is environmental benign as it employs polymer as ligands. It is envisaged that our work demonstrate the method for optimizing the shell material of recoverable magnetic Fe<sub>3</sub>O<sub>4</sub>

microparticles used for a series of reactions. It could enable further implications in a number of other application areas as well. We could infer our catalyst will have wonderful catalytic properties in other alcohols oxidation reactions.

## 5 Acknowledgements

The authors are grateful to Dr. Ren-Qi Wang for modification of the manuscript. The authors are grateful to the Key Laboratory of Nonferrous Metals Chemistry and Resources Utilization, Gansu Province for financial support.

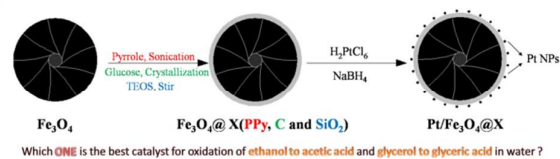
## 10 Notes and references

\*State Key Laboratory of Applied Organic Chemistry, College of Chemistry and Chemical Engineering, Lanzhou University, Lanzhou Gansu 730000, PR China. Corresponding author: Tel: +86-931-891-2577. Fax: +86-0931-891-2582 E-mail address: majiantai@lzu.edu.cn.

- 1 M. Besson, P. Gallezot and C. Pinel, *Chem. Rev.*, 2014, **114**, 1827.
- 2 (a) Y. Obana, H. Uchida and K. Sano, *US Pat.*, 6 867 164, 2005; (b) C. H. Christensen, B. Jørgensen, J. Rass-Hansen, K. Egeblad, R. Madsen, S. K. Klitgaard, S. M. Hansen, M. R. Hansen, H. C. Andersen and A. Riisager, *Angew. Chem. Int. Ed.*, 2006, **45**, 4648; (c) B. Jørgensen, S. E. Christiansen, M. L. D. Thomsen and C. H. Christensen, *J. Catal.*, 2007, **251**, 332; (d) V. I. Sobolev and K. Y. Koltunov, *ChemCatChem*, 2011, **3**, 1143.
- 3 (a) B. Katryniok, H. Kimura, E. Skrzyńska, J. S. Girardon, P. Fongarland, M. Capron, R. Ducoulombier, N. Mimura, S. Paul and F. Dumeignil, *Green Chem.*, 2011, **13**, 1960; (b) N. Dimitratos, J. A. Lopez-Sanchez, J. M. Anthonykutty, G. Brett, A. F. Carley, R. C. Tiruvalam, A. A. Herzing, C. J. Kiely, D. W. Knight and G. J. Hutchings, *Phys. Chem. Chem. Phys.*, 2009, **11**, 4952; (c) Z. Zhao, J. Arentz, L. A. Pretzer, P. Limpornpipat, J. M. Clomburg, R. Gonzalez, N. M. Schweitzer, T. P. Wu, J. T. Miller and M. S. Wong, *Chem. Sci.*, 2014, **5**, 3715; (d) C-H. Zhou, J. N. Beltramini, C-X. Lin, Z-P. Xu, G. Q. Lu and A. Tanksale, *Catal. Sci. Technol.*, 2011, **1**, 111; (e) Y. Y. Gorbanev, S. Kegnaes, C. W. Hanning, T. W. Hansen and A. Riisager, *ACS Catal.*, 2012, **2**, 604; (f) D. J. Tarnowski and C. Korzeniewski, *J. Phys. Chem. B*, 1997, **101**, 253; (g) J. C. Beltrán-Prieto, J. Pecha, V. Kašpárková and K. Kolomazník. *J. Liq. Chromatogr. R. T.*, 2013, **36**, 2758.
- 4 (a) H. Danner and R. Braun, *Chem. Soc. Rev.*, 1999, **28**, 395; (b) J. J. Spivey and A. Egbebi, *Chem. Soc. Rev.*, 2007, **36**, 1514; (c) H. de Lasa, E. Salaiques, J. Mazumder and R. Lucky, *Chem. Rev.*, 2011, **111**, 5404; (d) T. J. Morgan and R. Kandiyoti, *Chem. Rev.*, 2014, **114**, 1547; (e) A. J. J. Straathof, *Chem. Rev.*, 2014, **114**, 1871; (f) J. C. Colmenares and R. Luque, *Chem. Soc. Rev.*, 2014, **43**, 765; (g) D. M. Alonso, S. G. Wettstein and J. A. Dumesic, *Chem. Soc. Rev.*, 2012, **41**, 8075; (h) M. Besson, P. Gallezot and C. Pinel, *Chem. Rev.*, 2014, **114**, 1827.
- 5 (a) J. Jarupatrakorn, M. P. Coles and T. D. Tilley, *Chem. Mater.*, 2005, **17**, 1818; (b) Q. H. Yang, C. Copéret, C. Li and J. M. Basset, *New. J. Chem.*, 2003, **27**, 319; (c) R. Ghahremanzadeh, Z. Rashid, A.-H. Zarnani and H. Naeimi, *Dalton Trans.*, 2014, **43**, 15791.
- 6 (a) M. J. Jia, A. Seifert, W. R. Thiel, *Chem. Mater.*, 2003, **15**, 2174; (b) N. Narkhede, A. Patel and S. Singh, *Dalton Trans.*, 2014, **43**, 2512; (c) N. J. Hao, L. F. Li and F. Q. Tang, *J. Mater. Chem. A*, 2014, **2**, 11565.
- 7 (a) Y. J. Hong, X. Q. Yan, X. F. Liao, R. H. Li, S. D. Xu, L. P. Xiao and J. Fan, *Chem. Commun.*, 2014, **50**, 9679; (b) A. Primo and H. Garcia, *Chem. Soc. Rev.*, 2014, **43**, 7548; (c) A. Rojas and M. A. Cambor, *Dalton Trans.*, 2014, **43**, 10760.
- 8 (a) Z. Z. Jiang, Z. B. Wang, Y. Y. Chu, D. M. Gu and G. P. Yin, *Energy Environ. Sci.*, 2011, **4**, 2558; (b) K. Machado, J. Mishra, S. Suzuki and G. S. Mishra, *Dalton Trans.*, 2014, **43**, 17475; (c) J. W. Guo, B. Zhang, Y. Hou, S. Yang, X. H. Yang and H. G. Yang, *J. Mater. Chem. A*, 2013, **1**, 1982.

- 9 (a) J. D. Bass, A. Solovyov, A. J. Pascall and A. Katz, *J. Am. Chem. Soc.*, 2006, **128**, 3737; (b) R. Abu-Reziq, D. Wang, M. Post and H. Alper, *Chem. Mater.*, 2008, **20**, 2544; (c) Y. Q. Wang, B. F. Zou, T. Gao, X. P. Wu, S. Y. Lou and S. M. Zhou, *J. Mater. Chem.*, 2012, **22**, 9034; (d) W. Guo, C. Yang, H. Lin and F. Qu, *Dalton Trans.*, 2014, **43**, 18056; (e) V. Polshettiwar, R. Luque, A. Fihri, H. Zhu, M. Bouhrara, and J. M. Basset, *Chem. Rev.*, 2011, **111**, 3036; (f) J. Mondal, T. Sen and A. Bhaumik, *Dalton Trans.*, 2012, **41**, 6173; (g) M. Xie, F. W. Zhang, Y. Long and J. T. Ma, *RSC Adv.*, 2013, **3**, 10329; (h) W. Stöber, A. Fink and E. J. Bohn, *Colloid Interface Sci.*, 1968, **26**, 62; (i) D. Yang, J. H. Hu, and S. K. Fu, *J. Phys. Chem. C*, 2009, **113**, 7646; (j) Y. Long, B. Yuan, J. Niu, X. Tong and J. Ma, *New J. Chem.*, 2015, **39**, 1179; (k) D. Wang and D. Astruc, *Chem. Rev.* 2014, **114**, 6949; (l) R. B. N. Baig and R. S. Varma, *Chem. Commun.* 2013, **49**, 752; (m) C. W. Lim and I. S. Lee, *Nano Today* 2010, **5**, 412.
- 10 (a) F. H. Richter, Y. Meng, T. Klasen, L. Sahraoui and F. Schüth, *J. Catal.*, 2013, **308**, 341; (b) S. Carrettin, P. McMorn, P. Johnston, K. Griffin, C. J. Kiely and G. J. Hutchings, *Phys. Chem. Chem. Phys.*, 2003, **5**, 1329; (c) H. F. Wang and Z. P. Liu, *J. Am. Chem. Soc.*, 2008, **130**, 10996; (d) Y. Kwon, K. J. P. Schouten and M. T. M. Koper, *ChemCatChem*, 2011, **3**, 1176; (e) B. N. Zope, D. D. Hibbitts, M. Neurock and R. J. Davis, *Science*, 2010, **330**, 74.

## A table of contents entry



PPy coated magnetite microparticles immobilizing Pt nanoparticles was a highly-efficient catalyst for the selective aerobic oxidation of ethanol and glycerol